State-dependent diffusion in a bistable potential: Conditional probabilities and escape rates

Miguel V. Moreno,[1,*] Daniel G. Barci,[2,†] and Zochil González Arenas[3]

[1]*Instituto de de Física Teórica, Universidade Estadual Paulista, Rua Dr. Bento Teobaldo Ferraz 271, 01140-070 São Paulo, SP Brazil*

[2]*Departamento de Física Teórica, Universidade do Estado do Rio de Janeiro, Rua São Francisco Xavier 524, 20550-013, Rio de Janeiro, RJ, Brazil*

[3]*Departamento de Matemática Aplicada, IME, Universidade do Estado do Rio de Janeiro, Rua São Francisco Xavier 524, 20550-013, Rio de Janeiro, RJ, Brazil*

(Received 1 December 2019; revised manuscript received 5 May 2020; accepted 18 May 2020; published 2 June 2020)

We consider a simple model of a bistable system under the influence of multiplicative noise. We provide a path integral representation of the overdamped Langevin dynamics and compute conditional probabilities and escape rates in the weak noise approximation. The saddle-point solution of the functional integral is given by a diluted gas of instantons and anti-instantons, similar to the additive noise problem. However, in this case, the integration over fluctuations is more involved. We introduce a local time reparametrization that allows its computation in the form of usual Gaussian integrals. We found corrections to the Kramers escape rate produced by the diffusion function which governs the state-dependent diffusion for arbitrary values of the stochastic prescription parameter. Theoretical results are confirmed through numerical simulations.

DOI: 10.1103/PhysRevE.101.062110

I. INTRODUCTION

The physics of thermal or noise activation over a barrier has a long history. Nowadays, it is an important research topic because of the wide range of applications in several areas of science, such as physics, chemistry, and biology [1]. The simplest model to study this problem is a classical particle in a bistable potential, $U(x)$, whose dynamics is driven by an overdamped Langevin equation with additive white noise. In this context, an important physical quantity is the rate at which the particle escape out of a minimum of the potential. The seminal work of Kramers [2] stated the very simple formula

$$r_{\rm add} = \frac{\sqrt{\omega_{\rm min}|\omega_{\rm max}|}}{2\pi} e^{-\frac{\Delta U}{\sigma^2}}, \tag{1.1}$$

where $r_{\rm add}$ is the escape rate, $\Delta U = U(x_{\rm max}) - U(x_{\rm min})$ is the height of the potential barrier, σ^2 is the noise intensity, and $\omega_{\rm min} = U''(x_{\rm min})$ and $\omega_{\rm max} = U''(x_{\rm max})$ are the local curvatures of the potential at its minimum ($x_{\rm min}$) and its maximum ($x_{\rm max}$), respectively (primes mean derivative with respect to x). We use the notation $r_{\rm add}$ to emphasize that this expression for the escape rate was computed assuming an *additive noise* stochastic differential equation. Equation (1.1) is valid in the weak noise or high barrier approximation $\sigma^2 \ll \Delta U$. Since this well-established result was defined, a lot of work has been done in order to compute more accurate expressions suitable to be applied to more realistic situations. The generalization of Eq. (1.1) to multidimensional systems was (and still is) a big challenge [3]. Moreover, generalizations to different types of noise probability distributions have been also considered [4–9].

On the other hand, there is increasing interest for multiplicative noise stochastic systems. Some examples of multiplicative noise dynamics are given by the diffusion of particles near a wall [10–14], micromagnetic dynamics [15–17], and nonequilibrium transitions into absorbing states [18]. There are two particular stochastic phenomena in which multiplicative noise plays an important role: noise-induced phase transitions [19–23] and stochastic resonance [24–27]. In the last case, the escape rate is at the stem of the physical description of the observed phenomenology.

One of the main questions that we address in this paper is how the Kramers escape rate of Eq. (1.1) is modified when the dynamics is driven by a general multiplicative noise, modeled by a diffusion function $g(x)$. This topic rarely has been treated in the past and there is some controversy in the literature [28–32]. In particular, we study the dependence of the escape rate on the stochastic prescription, necessary to correctly define the multiplicative noise Langevin equation. This point is particularly relevant in order to compare analytic results with numerical simulations. Our main result is

$$r_{\rm mult} = g^2(x_{\rm max}) \frac{\sqrt{\tilde{\omega}_{\rm min}|\tilde{\omega}_{\rm max}|}}{2\pi} e^{-\frac{\Delta U_{\rm eq}}{\sigma^2}}. \tag{1.2}$$

We used the notation $r_{\rm mult}$ to denote the escape rate in the *multiplicative noise* case. In general, we observe that the Arrhenius form of the Kramers result still remains. Another similarity with Eq. (1.1) is that the escape rate does not depend on details, either of the potential or of the diffusion function. Instead, it only depends on the local properties of these functions at the maximum and minima of the potential. On the other hand, there are significant differences

*Previously at: Departamento de Física, Universidade Federal Fluminense and National Institute of Science and Technology for Complex Systems, Av. Gal. Milton Tavares de Souza s/n, Campus da Praia Vermelha, 24210-346 Niterói, RJ, Brazil.

†Corresponding author: daniel.barci@gmail.com

between both results. First, the original potential $U(x)$ has been replaced by the equilibrium potential $U_{\rm eq}(x)$, obtained from the solution of the asymptotic stationary Fokker-Planck equation [Eq. (2.5)]. This potential depends on the noise and, more importantly, on the prescription used to interpret the stochastic differential equation. The barrier height is, in this case, $\Delta U_{\rm eq} = U_{\rm eq}(x_{\rm max}) - U_{\rm eq}(x_{\rm min})$. It is worth noting that $x_{\rm max}$ and $x_{\rm min}$ are the positions of the maximum and minimum of the equilibrium potential $U_{\rm eq}$ and not of the original "classical" potential $U(x)$. Local curvatures $\tilde{\omega}_{\rm min} = U''_{\rm eq}(x_{\rm min})$ and $\tilde{\omega}_{\rm max} = U''_{\rm eq}(x_{\rm max})$ are also computed by using the equilibrium potential. Finally, there is an overall factor given by the diffusion function computed at the maximum of the equilibrium potential, $g^2(x_{\rm max})$, coming from a careful treatment of fluctuations. We describe the model and the technique used to compute Eq. (1.2), discussing the result in more detail throughout the paper.

Multiplicative stochastic processes can be studied with different theoretical approaches. For numerical simulations [33], the Langevin approach seems to be more adequate. The Fokker-Planck equation is perhaps more appropriate to develop analytic calculations, especially in the long time stationary limit. In this context, techniques such as mean fields, perturbation theory, and even renormalization groups are also available [34]. On the other hand, the path integral formulation of stochastic processes is the more natural technique to compute correlation and response functions [35]. Important progress has been recently reached in the path integral representation of multiplicative noise processes [36–41], despite the fact that this topic has been studied for a long time [42].

The escape rate is just one ingredient of a more general problem that is the computation of conditional probabilities. Equilibrium properties, such as detailed balance, can be cast in terms of the conditional probability and its time reversal. Time-reversal transformations, detailed balance relations, as well as microscopic reversibility in multiplicative processes were studied in detail in Ref. [39]. More recently, we have presented a useful path integral technique to compute weak noise expansions [43]. The integration over fluctuations in the multiplicative case is not trivial. The reason is that the diffusion function produces an integration measure that resembles a curved time axis [44]. We have provided a local time reparametrization in order to integrate fluctuations [43]. In this paper, we compute the conditional probability of finding a particle in a well at large times $t/2$, provided it was in the same or the other well at $-t/2$. In the weak noise approximation, saddle points provide a set of diluted instanton and anti-instanton solutions. The diluted instanton gas approximation was first introduced in the context of quantum mechanics to compute the tunneling probability across a potential barrier [45]. In the context of an additive stochastic process, it was developed in great detail in Refs. [46,47]. From a technical point of view, we generalize the calculation of Ref. [47] to the multiplicative noise case, using the time reparametrization techniques introduced in Ref. [43]. We also perform extensive Langevin simulations to test our results and approximations, finding excellent agreement.

The paper is organized as follows. In the next section, we present the equilibrium properties of a particle in a double-well potential under state-dependent diffusion. In Sec. III, we briefly review the path-integral representation of a conditional probability in a multiplicative process and we show, in Sec. IV, how to integrate fluctuations. We develop the dilute instanton gas approximation in Sec. V, where we compute conditional probabilities and the escape rate. In Sec. VI, we present Langevin simulations of a particular model and compare the output with our analytic results. Finally, we discuss our results in Sec. VII. We leave to the Appendix some details of the calculation.

II. EQUILIBRIUM PROPERTIES OF A PARTICLE IN A DOUBLE-WELL POTENTIAL UNDER STATE-DEPENDENT DIFFUSION

In this section, we describe the equilibrium properties of a model consisting of a single particle in a double-well potential coupled with a thermal bath with state-dependent diffusion. We consider a conservative one-dimensional system described by a potential energy $U(x) = U(-x)$ with a double minima structure. The thermal bath is characterized by the diffusion function $g(x) = g(-x)$. The reflection symmetry $x \to -x$ is not essential and most of our results do not depend on it. However, to keep the discussion as simple as possible, we focus on the symmetric model, leading the details of a more general asymmetric situation to a future presentation.

In order to reach thermodynamic equilibrium at long times, the drift force $f(x)$ should be related with the classical potential $U(x)$ through a generalized Einstein relation [38,39]:

$$f(x) = -\frac{1}{2} g^2(x) \frac{dU(x)}{dx} \,. \tag{2.1}$$

In this way, the overdamped stochastic dynamics is driven by the Langevin equation

$$\frac{dx}{dt} = -\frac{1}{2} g^2(x) \frac{dU(x)}{dx} + g(x)\eta(t), \tag{2.2}$$

where $\eta(t)$ obeys a Gaussian white noise distribution with

$$\langle \eta(t) \rangle = 0 \;\;, \;\; \langle \eta(t)\eta(t') \rangle = \sigma^2 \delta(t - t') \,, \tag{2.3}$$

in which σ^2 measures the noise intensity. This equation is understood in the *generalized Stratonovich* [48] prescription (also known as the α prescription [42]). The asymptotic long time equilibrium probability distribution is given by [39]

$$P_{\rm eq}(x) = \mathcal{N}\, e^{-\frac{1}{\sigma^2} U_{\rm eq}(x)}, \tag{2.4}$$

where $\mathcal{N}$ is a normalization constant and the equilibrium potential

$$U_{\rm eq}(x) = U(x) + (1 - \alpha)\sigma^2 \ln g^2(x) \,. \tag{2.5}$$

The parameter $0 \leqslant \alpha \leqslant 1$ labels the particular stochastic prescription used to discretize the Langevin equation. For instance, $\alpha = 0$ corresponds with the Itô interpretation while $\alpha = 1/2$ corresponds with the Stratonovich one. In this way, the equilibrium potential is not the bare classical potential, but it is corrected by the diffusion function $g(x)$. On the other hand, the case $\alpha = 1$ corresponds with Hänggi-Klimontovich or kinetic interpretation [49,50]. This is the only prescription which leads to the Boltzmann distribution $U_{\rm eq}(x) = U(x)$. Furthermore, this prescription is also known as anti-Itô and

can be considered as the time reversal conjugated to the Itô prescription [39,40].

Although the techniques and results of this paper do not depend on details, either of $U(x)$ or of $g(x)$, it is convenient, just to visualize the equilibrium potential $U_{\rm eq}(x)$, to consider a very simple model. Let us take, for instance,

$$U(x) = -\tfrac{1}{2}x^2 + \tfrac{1}{4}x^4 \,, \tag{2.6}$$

with the diffusion function

$$g(x) = 1 + \lambda x^2, \tag{2.7}$$

where the parameter λ measures in some sense the multiplicative character of the noise. The particular value of $\lambda = 0$ corresponds with an additive noise. The potential $U(x)$ has two degenerated minima at $x_{\rm min} = \pm 1$ and a local maximum at $x_{\rm max} = 0$. The contribution of the multiplicative noise for the equilibrium potential is quite interesting. In the weak noise limit, the global two-minima structure remains the same. However, the minima are displaced to

$$\begin{aligned} x_{\rm min} &= \pm[1 - 4\sigma^2(1-\alpha)]^{1/4} \\ &\sim \pm 1 \mp \sigma^2(1-\alpha) + O(\sigma^4) \,. \end{aligned} \tag{2.8}$$

For $\sigma^2 \geqslant 1/4(1-\alpha)$, both minima melt in a single one, deeply changing the global structure of the potential. This dependence on the noise intensity resembles a second-order phase transition, where the critical noise is given by

$$\sigma_c = \frac{1}{2}\frac{1}{\sqrt{1-\alpha}} \,. \tag{2.9}$$

Interestingly, the critical noise depends on the stochastic prescription. For $\alpha \to 1$, $\sigma_c \to \infty$, meaning that, in the anti-Itô prescription, the double-well structure is preserved for all values of the noise.

In Fig. 1, we depict the equilibrium potential $U_{\rm eq}(x)$ given by Eq. (2.5) for the simple model specified by Eqs. (2.6) and (2.7), for different values of the parameters σ and α. In Fig. 1(a), we show the equilibrium potential for $\sigma = 0.5$ and different values of the stochastic prescription $\alpha = 0, 1/2, 1$. We see that, for $\alpha = 1$, $U_{\rm eq} = U$ and the minima are fixed at $x_{\rm min} = \pm 1$. However, in the Stratonovich and Itô prescriptions, the minima are displaced toward the origin. In Fig. 1(b), the three curves are computed in the Itô prescription with different values of the noise $\sigma = 1/5, 2/5, 2/3$. In this case, the minima approach zero when the noise grows and, for the value $\sigma = 2/3 > \sigma_c = 1/2$, the equilibrium potential has only one global minimum at $x_{\rm min} = 0$.

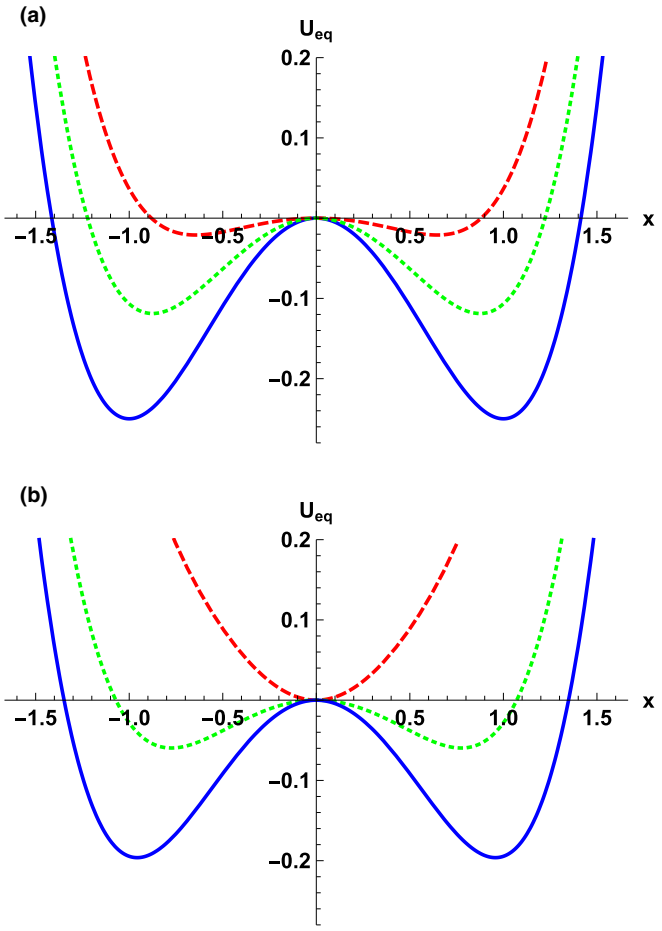

FIG. 1. Equilibrium potential $U_{\rm eq}(x)$ given by Eq. (2.5). In panel (a), we fixed $\sigma = 0.5$. The continuous line is plotted in the anti-Itô prescription $\alpha = 1$, the dotted line is in the Stratonovich prescription $\alpha = 1/2$ and the dashed line corresponds to the Itô interpretation $\alpha = 0$. In panel (b), all the curves are computed in the Itô interpretation. The continuous curve is plotted with $\sigma = 1/5$, the dotted line with $\sigma = 2/5$, and the dashed line with $\sigma = 2/3$. In both figures, we have fixed $\lambda = 1$.

III. CONDITIONAL PROBABILITIES: PATH INTEGRAL REPRESENTATION

We are interested in computing the conditional probability $P(x_f, t_f|x_i, t_i)$ of finding the system in the state x_f at time t_f, provided the system was in the state x_i at a previous time t_i. It is useful to express this quantity using a path integral representation [43]. It can be written as

$$P(x_f, t_f|x_i, t_i) = e^{-\frac{\Delta U_{\rm eq}}{2\sigma^2}} K(x_f, t_f|x_i, t_i), \tag{3.1}$$

where $\Delta U_{\rm eq} = U_{\rm eq}(x_f) - U_{\rm eq}(x_i)$ and the *propagator* $K(x_f, t_f|x_i, t_i)$ is given by

$$K(x_f, t_f|x_i, t_i) = \int [\mathcal{D}x]\; e^{-\frac{1}{\sigma^2}\int_{t_i}^{t_f} dt\; L(x,\dot{x})} \,. \tag{3.2}$$

Here, the functional integration measure is

$$[\mathcal{D}x] = \mathcal{D}x \det{}^{-1} g = \lim_{\substack{N\to\infty \\ \Delta t \to 0}} \prod_{n=0}^{N} \frac{dx_n}{\sqrt{\Delta t\; g^2\left(\frac{x_n + x_{n+1}}{2}\right)}}, \tag{3.3}$$

where $x_0 = x_i$ and $x_N = x_f$. The Lagrangian can be written in the form

$$L = \frac{1}{2}\left(\frac{1}{g^2(x)}\right)\dot{x}^2 + V(x) \,, \tag{3.4}$$

where

$$V(x) = \frac{g^2}{2}\left[\left(\frac{U'_{\rm eq}}{2}\right)^2 - \sigma^2\left(\frac{U''_{\rm eq}}{2} + \frac{g'}{g}U'_{\rm eq}\right)\right] + \frac{\sigma^4}{4}(gg')' . \tag{3.5}$$

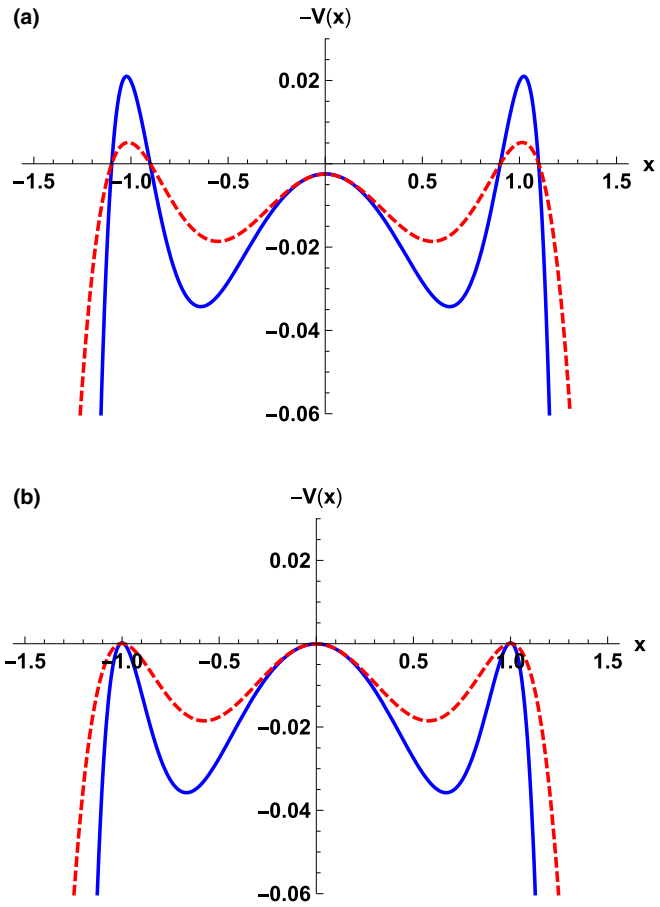

FIG. 2. Potential $-V(x)$ given by Eq. (3.5). All the plots are in the Itô prescription, $\alpha = 0$. The dashed lines are the potentials in the additive noise case $g(x) = 1$ and the continuous lines correspond with multiplicative noise, for $g(x) = 1 + x^2$. In panel (a), we have fixed $\sigma = 0.1$ while in panel (b), $\sigma = 0.01$.

The primes mean derivative with respect to x. Equation (3.2), with the Lagrangian defined by Eq. (3.4), correctly describes the dynamics of the Langevin Eq. (2.2) for arbitrary values of the parameter $0 \leqslant \alpha \leqslant 1$ [43]. It is important to note that all the information about the stochastic prescription is codified in the structure of the equilibrium potential $U_{\rm eq}(x)$, contained in the definition of the potential $V(x)$, Eq. (3.5). In this particular representation, the path integral measure given by Eq. (3.3) is discretized symmetrically, allowing us to use normal calculus rules in the manipulation of the path integral (for more details on the subtleties of stochastic calculus in the path integral formulation, please see Ref. [39] and references therein).

An interesting observation is that Eq. (3.2) coincides with the propagator of a quantum particle with position-dependent mass $m(x) = 1/g^2(x)$ moving in a potential $V(x)$, written in the imaginary time path integral formalism $t \to -it$. The noise σ^2 plays the role of $\hbar$ in the quantum theory. At a classical level, the Lagrangian, Eq. (3.4), represents a particle with variable mass moving in a potential $-V(x)$. The structure of the potential $-V(x)$ [Eq. (3.5)] is much more complex than $U(x)$ or even $U_{\rm eq}(x)$.

In Fig. 2, we plotted the potential $-V(x)$ for the simple model displayed by Eq. (2.6). All the curves have been plotted in the Itô prescription $\alpha = 0$. The dashed lines correspond to the additive noise case $g(x) = 1$, while the continuous lines represent the potential in the multiplicative noise case, with $g(x) = 1 + x^2$. In Fig. 2(a), we fixed $\sigma = 0.1$, while in Fig. 2(b), $\sigma = 0.01$. The first observation is that $-V(x)$ has three maxima and two minima. The location of both nonzero maxima roughly coincides with the minima of the potential $U(x)$. The difference is of the order of σ^2. The main effect of the diffusion function is to increase the curvature at each maxima with a factor proportional to $g^2(x_{\rm max}) > 1$. An important feature that will be relevant to compute conditional probabilities is that the difference between the height of the peaks are of the order of σ^2. Thus, in a weak noise regime, the difference between the three maxima tends to disappear. In the extreme limit of $\sigma \to 0$, the potential $-V(x)$ has three degenerate maxima. This fact is clearly shown in Fig. 2(b). It is timely to note that the structure of $-V(x)$ is quite different from a similar calculus of the tunneling probability amplitude of a quantum particle [45]. In that case, the relevant potential is $-U(x)$, which has only two maxima. The appearance of a quasidegenerate maximum at $x = 0$ is proper of a classical stochastic process, even additive as well as multiplicative.

IV. FLUCTUATIONS AND TIME REPARAMETRIZATION

The usual weak noise expansion consists in evaluating the path integral of Eq. (3.2) in the saddle-point approximation plus Gaussian fluctuations. Generally, multiplicative noise induces an integration measure that depends on the diffusion function $g(x)$. In Ref. [43], we have shown how to overcome this problem by means of a time reparametrization. In this section, we briefly review this technique since we will use it to compute conditional probabilities.

The classical equation of motion is

$$\frac{d^2x}{dt^2} = g^2V' + \frac{g'}{g}\dot{x}^2 \,. \tag{4.1}$$

Despite the fact that this is a complicated nonlinear equation, using time translation symmetry, a first integral can be built up. We have

$$\dot{x}_{cl}^2 = 2g_{cl}^2(V_{cl} + H) \,. \tag{4.2}$$

Here, $x_{cl}(t)$ is a solution of Eq. (4.1). The notation x_{cl} stands for classical solution, resembling in some sense a semiclassical calculation in quantum mechanics. H is an arbitrary constant, $g_{cl} = g(x_{cl}(t))$ and $V_{cl} = V(x_{cl}(t))$. Then, the solution of Eq. (4.1) can be expressed by a quadrature

$$t - t_0 = \int_0^{x_{cl}} \frac{ds}{\sqrt{2V_{\rm eff}(s)}} \,, \tag{4.3}$$

where we have defined an effective potential,

$$V_{\rm eff}(x) = g^2(x)[V(x) + H]. \tag{4.4}$$

These expressions have two arbitrary constants, t_0 and H, that should be determined by means of the boundary conditions $x_{cl}(t_i) = x_i$ and $x_{cl}(t_f) = x_f$. Thus, Eqs. (4.3) and (4.4) implicitly define $x_{cl}(t)$, used as a starting point of the weak noise approximation.

Let us assume, for the moment, that, given initial and final conditions, the classical solution x_{cl} is unique. Then, we consider fluctuations around it

$$x(t) = x_{cl}(t) + \delta x(t)\,, \tag{4.5}$$

with boundary conditions $\delta x(t_i) = \delta x(t_f) = 0$. Putting Eq. (4.5) into Eq. (3.2) and keeping up to second-order terms in the fluctuations, we find for the propagator

$$K(x_f, t_f|x_i, t_i) = e^{-\frac{1}{\sigma^2}S_{cl}} \int [\mathcal{D}\delta x]\; e^{-\frac{1}{2}\int dt dt'\; \delta x(t) O(t,t') \delta x(t')}, \tag{4.6}$$

where the classical action S_{cl} is

$$S_{cl} = \int_{t_i}^{t_f} dt\; L(x_{cl}(t), \dot{x}_{cl}(t)) \tag{4.7}$$

and the fluctuation kernel,

$$O(t,t') = -\frac{d}{dt}\left[\frac{1}{g_{cl}^2}\frac{d\delta(t-t')}{dt}\right] + \left[\frac{1}{g_{cl}^2}V'_{\rm eff}(x_{cl})\right]'\delta(t-t'). \tag{4.8}$$

In Eq. (4.6), the functional integration measure is

$$[\mathcal{D}\delta x] = \lim_{\substack{N\to\infty \\ \Delta t\to 0}} \prod_{n=0}^{N} \frac{d\delta x_n}{\sqrt{\Delta t\; g^2\left(\dfrac{x_{cl}(t_n) + x_{cl}(t_{n+1})}{2}\right)}}. \tag{4.9}$$

Due to the time dependence of $g_{cl} = g(x_{cl}(t))$, the fluctuation kernel $O(t,t')$ is not trivial. On the other hand, the integration measure, Eq. (4.9), depends on the diffusion function $g(x(t))$. As a consequence, although the exponent in Eq. (4.6) is quadratic, the evaluation of the functional integral is cumbersome. In this case, to compute the fluctuation integral, we make a time reparametrization. For concreteness, we introduce a new time variable τ by means of

$$\tau = \int_0^t g^2(x_{cl}(t'))dt'\,. \tag{4.10}$$

This is a nontrivial *local* scale transformation, weighted by the diffusion function evaluated at the classical solution $x_{cl}(t)$. Performing this time reparametrization, the fluctuation kernel transforms as $O(t,t') \to \Sigma(\tau,\tau')$ and takes the simpler form

$$\Sigma(\tau,\tau') = \left[-\frac{d^2}{d\tau^2} + W[x_{cl}]\right]\delta(\tau-\tau'), \tag{4.11}$$

where

$$W(x_{cl}) = \frac{1}{g_{cl}^2}\left[\frac{1}{g_{cl}^2}V'_{\rm eff}(x_{cl})\right]'. \tag{4.12}$$

More important, after discretizing the reparametrized time axes τ, the functional integration measure, Eq. (4.9) becomes

$$[\mathcal{D}\delta x] = \lim_{\substack{N\to\infty \\ \Delta\tau\to 0}} \prod_{n=0}^{N} \frac{d\delta x_n}{\sqrt{\Delta\tau}}\,, \tag{4.13}$$

in which the function $g(x_{cl})$ has been absorbed in the reparametrization.

Thus, in the new time variable τ, the functional integral over fluctuations can be formally evaluated, obtaining for the propagator

$$K(x_f, t_f|x_i, t_i) = [\det \Sigma(\tau_i, \tau_f)]^{-1/2} e^{-\frac{1}{\sigma^2}S_{cl}(t_i,t_f)}\,, \tag{4.14}$$

where the relation between (τ_i, τ_f) and (t_i, t_f) is given through Eq. (4.10).

Equation (4.14) is formally similar to the weak noise expansion in the additive noise case. However, in this case, the determinant is written in terms of a rescaled time parameter τ. Thus, in order to compute a prefactor, we need to reparametrized the time variable, compute the determinant and, at the end, go back to the original time. In Ref. [43], we have successfully used this technique to compute conditional probabilities of an harmonic oscillator in a multiplicative noise environment. Here, we will use it to compute conditional probabilities in a double-well setup.

V. PROBABILITY OF REMAINING IN A WELL

In order to compute conditional probabilities, let us consider a potential $-V(x)$ with the general structure displayed in Fig. 2. We will consider that the potential has local maxima at $x = \pm a$ and $x = 0$, while it has two minima, at $x = \pm x_p$. The difference $|V(a) - V(0)| \sim O(\sigma^2)$, in such a way that the three maxima are degenerated in the limit $\sigma \to 0$. As we have mentioned, the maxima at $x = \pm a$ roughly coincide with the minima of the bare potential $U(x)$. The difference is of order σ^2.

We want to compute the probability of remaining in a minimum of $U(x)$, after some time t. Let us compute, for instance, the probability of remaining in the state $x = -a$, i.e., the probability of finding the particle in the state $x = -a$ at a time $t/2$, provided it was in the same point, at a time $-t/2$. As the initial and final states coincide, $\Delta U_{\rm eq} = 0$ and, from Eq. (3.1), we see that this conditional probability coincides with the propagator, $P(-a, t/2| - a, -t/2) = K(-a, t/2| - a, -t/2)$. So, we are interested in the function $K(-a, -t/2 \,| - a, t/2)$ for very long times, $t \to \infty$.

The main point is that for long times, there are a huge number of solutions (or approximate solutions) of the saddle-point equation which need to be considered in order to compute the path integral in the weak noise approximation. A trivial solution of Eq. (4.1) with initial and final conditions $x_{cl}(-t/2) = x_{cl}(t/2) = -a$ is simply $x_{cl} = -a$. In this case, the multiplicative noise has a trivial effect. Since x_{cl} does not depend on time, the diffusion function g_{cl} is a simple constant that renormalizes the noise intensity σ. Then, the contribution of this solution to $K(-a, t/2| - a, -t/2)$ can be easily computed, obtaining

$$K^{(0)}(-a, t/2| - a, -t/2) = \left[\frac{g_a^2 U''_{\rm eq}(a)}{2\pi\sigma^2}\right]^{1/2}, \tag{5.1}$$

where $g_a = g(a)$. We are using the superscript (0) to indicate the contribution of the constant solution to the propagator.

A. Instantons/anti-instantons

In the case of potentials with two degenerate maxima, there are topological time-dependent solutions of the equation of

motion with finite action that interpolate between both maxima. These solutions are called instantons or anti-instantons and should be taken into account to compute the propagator. For very large time intervals, well-separated superposition of instantons and anti-instantons will also contribute to the path integral in a nontrivial way. The technique of summation over these configurations, usually called instanton/anti-instanton diluted gas approximation, was developed by several authors to compute tunneling amplitudes in quantum mechanics [45,51,52]. In stochastic processes, the technique was applied to the case of additive white noise in Ref. [47], in which the problem of a diffusion in a bistable potential was addressed. Some years later, the same technique was successfully applied to color noise processes [4–7]. Here, we will apply it to the multiplicative noise case. In the rest of this section, we will closely follow the calculation of Ref. [47], emphasizing those steps that are proper of multiplicative noise.

In addition to the constant solution, there are other time-dependent trajectories which begin and end at $x = -a$ for very long time intervals that will contribute to the propagator. In our case, the maximum at $x = 0$ is quasidegenerate with $x = \pm a$. For this reason, we expect that trajectories which begin at $x = -a$, go to approximately $x = 0$, and then return to the original point will also have an important weight in the functional integral. These types of trajectories are not exact solutions of the classical equation of motion, so then there will be a linear term in the fluctuation expansion. However, this term will be $O(\sigma^2)$ since, in the limit $\sigma \to 0$, it should disappear.

We denote by $K^{(1)}(-a, t/2| - a, -t/2)$ the contribution of the trajectory $-a \to 0 \to -a$ to the propagator. To compute it, we first rewrite the Lagrangian, Eq. (3.4), in the following way:

$$L = \frac{1}{2}\left(\frac{1}{g^2(x)}\right)\dot{x}^2 + V^{(0)}(x) + \delta V(x)\,, \tag{5.2}$$

where we have defined the quantity

$$\delta V(x) = V(x) - V^{(0)}(x) = \begin{cases} 0, & x < -x_p \\ V_0 - V_a, & x > -x_p \end{cases}. \tag{5.3}$$

In the last expression, $-x_p$ is the position of the minimum of the potential $-V(x)$, $V_a = V(a) = V(-a)$ and $V_0 = V(0)$. The specific form of $\delta V(x)$, as well as the specific value x_p are not important. The final results will not depend on such details. Thus, the first two terms of Eq. (5.2) describe the dynamics of a particle in a potential $-V^{(0)}$ with truly degenerate maxima, while $\delta V(x) \sim O(\sigma^2)$.

Let us compute asymptotic solutions of the classical equation of motion for the potential $-V^{(0)}$. We define the instanton, $x_I(t)$, as the solution with initial and final conditions $x_{cl}(-t/2) = -a$ and $x_{cl}(t/2) = 0$, for very large values of t. From Eq. (4.3), we have

$$t - t_0 = \int_{-x_p}^{x_I} \frac{dx}{\sqrt{2g^2(x)(V^{(0)}(x) - V_a)}}\,, \tag{5.4}$$

where we fixed the conditions $x_I(t_0) = -x_p$ and $H = V_a$. These parameters guarantee the above-mentioned initial and final conditions.

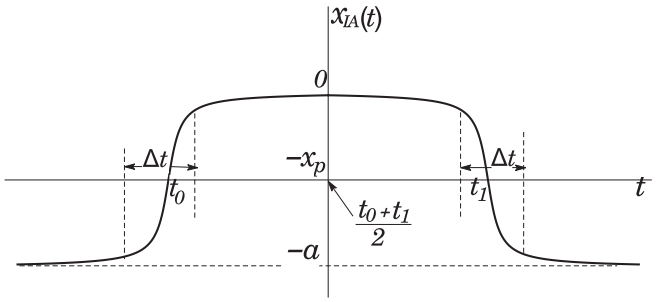

FIG. 3. Instanton/anti-instanton pair trajectory in the potential $-V^{(0)}(x)$.

We see, from Eq. (5.4), that the integral is dominated by the region in which $V^{(0)}(x) - V_a \to 0$. It happens for $x \to 0 > -x_p$ or $x \to -a < -x_p$. Thus, to compute the integral we can expand $V^{(0)}(x)$ around $x = 0$ and $x = -a$ to second order in powers of x and $x + a$, respectively. Thus, in the harmonic approximation we have

$$V_h^{(0)}(x) = \begin{cases} V_a + \frac{1}{2}V_0''x^2, & x > -x_p \\ V_a + \frac{1}{2}V_a''(x+a)^2, & x < -x_p \end{cases}. \tag{5.5}$$

Using this approximation, we obtain for the instanton solution

$$x_I(t) \underset{t \ll t_0}{\sim} -a + (-x_p + a)\, e^{g_a (V_a'')^{1/2}(t - t_0 - \Delta_{ap})}\,, \tag{5.6}$$

$$x_I(t) \underset{t \gg t_0}{\sim} -x_p\, e^{-g_0 (V_0'')^{1/2}(t - t_0 - \Delta_{0p})}\,, \tag{5.7}$$

where we have introduced the finite constants

$$\Delta(x_i, x_j) = \int_{x_i}^{x_j} \frac{dx}{\sqrt{2}}\left[\frac{1}{g(x)\sqrt{V^{(0)} - V_a}} - \frac{1}{g(x_i)\sqrt{V_h^{(0)} - V_a}}\right], \tag{5.8}$$

in such a way that, in Eq. (5.7), $\Delta_{0p} = \Delta(0, x_p)$ and $\Delta_{ap} = \Delta(a, x_p)$.

The instanton/anti-instanton pair of trajectories, corresponding with the path $-a \to 0 \to -a$, can be written as

$$x_{IA}(t, t_0, t_1) = \begin{cases} x_I(t - t_0), & t < \frac{t_0 + t_1}{2} \\ x_I(t_1 - t), & t > \frac{t_0 + t_1}{2} \end{cases}, \tag{5.9}$$

where $x_I(t)$ is given by Eqs. (5.6) and (5.7). A typical instanton/anti-instanton trajectory is shown in Fig. 3. The classical action is computed by replacing Eq. (5.9) into Eq. (5.2) and integrating in time between $t_i = -t/2$ and $t_f = t/2$. We find

$$\begin{aligned} S_{IA}(t, t_0, t_1) = {} & (V_0 - V_a)(t_1 - t_0) + V_a t \\ & - \frac{x_p^2 (V_0'')^{1/2}}{g_0} e^{g_0 (V_0'')^{1/2}(t_0 - t_1 + 2\Delta_{0p})} + U_{\rm eq}(0) \\ & - U_{\rm eq}(a) + \sigma^2 \ln\left|\frac{U_{\rm eq}''(a)\, g_a^2\, (x_p + a)}{U_{\rm eq}''(0)\, g_0^2\, x_p}\right| \\ & + \frac{\sigma^2}{2}\left[g_a^2 U_{\rm eq}''(a)\Delta_{pa} + g_0^2 U_{\rm eq}''(0)\Delta_{0p}\right], \end{aligned} \tag{5.10}$$

where we have used the notation $S_{IA} = S_{cl}[x_{IA}]$, i.e., the classical action computed at the instanton/anti-instanton configuration of Eq. (5.9).

The next step is to compute fluctuations around the instanton/anti-instanton solution. After the time reparametrization given by Eq. (4.10), we are lead to the computation of the determinant $\det \hat{\Sigma}(\tau_f, \tau_i)$, where the operator $\hat{\Sigma}$ is given by Eq. (4.11), evaluated at $x_{cl} = x_{IA}(\tau)$. Due to time translation invariance, the determinant has zero modes. Similarly to the original computation of instanton fluctuations [45], we need to properly take into account translation modes, identifying translation fluctuations with the integration over the collective variables t_0 and t_1. We obtain (see the Appendix)

$$K^{(1)}\left(-a, \frac{t}{2}\middle| -a, -\frac{t}{2}\right) = \mathcal{N}\int_{-t/2}^{t/2} dt_0 \int_{t_0}^{t/2} dt_1 \times g_a\sqrt{S_I}\, g_0 \sqrt{S_A}[\det{}' \hat{\Sigma}(\tau_f, \tau_i)]^{-1/2} \times e^{-\frac{1}{\sigma^2}S_{IA}(t, t_0, t_1)}, \tag{5.11}$$

where $S_I = S_{cl}[x_I]$, $S_A = S_{cl}[x_A]$, and the prime in the determinant indicates that it should be evaluated excluding the zero modes. We use the notation $K^{(1)}$ to indicate the contribution of the path $-a \to 0 \to -a$ to the propagator. This result is similar to the additive noise case [47]. The main difference is that the determinant is computed in a reparametrized time and the integration over collective variables t_0 and t_1 are renormalized by the diffusion function. The advantage of the reparametrized time is that the operator $\hat{\Sigma}$ has the simpler form of Eq. (4.11) and can be computed using the Gelfand-Yaglom theorem [53]. At the end of the calculation, we go back to the original time axes. Following tedious but usual procedures, we finally find

$$K^{(1)}\left(-a, \frac{t}{2}\middle| -a, -\frac{t}{2}\right) = -g_0^2 t\, K^{(0)}\, \Gamma\,, \tag{5.12}$$

where $K^{(0)}$ is the contribution of the constant solution, given by Eq. (5.1), and

$$\Gamma = \frac{[U''_{\rm eq}(a)|U''_{\rm eq}(0)|]^{1/2}}{2\pi} \exp\left\{-\frac{U_{\rm eq}(0) - U_{\rm eq}(a)}{\sigma^2}\right\}. \tag{5.13}$$

We see that the contribution of an instanton/anti-instanton configuration to the propagator at long times is a linear function of time. The structure of the coefficient Γ is very interesting. All the information about the stochastic calculus is hidden in the definition of the equilibrium potential, $U_{\rm eq}$. On the other hand, it does not depend on the details of $U_{\rm eq}(x)$, but instead it depends on the barrier height, $U_{\rm eq}(a) - U_{\rm eq}(0)$, and on the curvature at each maxima, $U''_{\rm eq}(0)$ and $U''_{\rm eq}(a)$. These properties are quite similar with the additive noise case, except for the fact that the original potential $U(x)$ is replaced by the equilibrium potential $U_{\rm eq}$ and the time is rescaled by the diffusion function at the maximum of the potential $t \to g_0^2 t$. In this way, $K^{(1)}$ does not depend on the details of $g(x)$, but only on its value at the maxima, $g(0)$ and $g(a)$.

Because of the structure of the potential $-V(x)$, there are other trajectories which contribute in a nontrivial way to the propagator; for instance, trajectories that begin in $x = -a$, go to $x = a$ passing through $x = 0$, and return to $x = -a$.

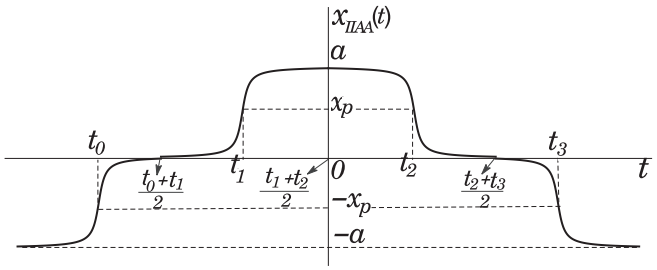

FIG. 4. Representation of a trajectory of 2-instanton and 2-anti-instanton in the potential $-V^{(0)}(x)$.

This kind of trajectories contains two instantons and two anti-instantons, as shown in Fig. 4. The contribution of these trajectories to the propagator can be computed following the same steps of the computation of the single instanton/anti-instanton case. We find, in this case,

$$K^{(2)}\left(-a, \frac{t}{2}\middle| -a, -\frac{t}{2}\right) = \frac{(g_0^2 t)^2}{2!}\, K^{(0)}\, \Gamma^2\,. \tag{5.14}$$

Thus, trajectories of the type $-a \to a \to -a$, produce a quadratic time contribution, the coefficient is simply Γ^2, where Γ is given by Eq. (5.13).

B. Kramers escape rate and time-reversal transformation

To compute the conditional probability of remaining in a minimum after some time t, we need to sum up all the trajectories that begin and end at $x = -a$ and which contribute to the propagator in a nontrivial way. Having in mind that $\Delta U_{\rm eq} = 0$, this probability coincides with the propagator, $P(-a, t/2| -a, -t/2) = K(-a, t/2| -a, -t/2)$. As described above, there are essentially three contributions to these paths: a constant one, $K^{(0)}$, given by Eq. (5.1), a linear term $K^{(1)}$ given by Eq. (5.12), corresponding to trajectories $-a \to 0 \to -a$ or, by symmetry, to $a \to 0 \to a$, and, finally, a quadratic term $K^{(2)}$ given by Eq. (5.14), related to the path $-a \to a \to -a$.

Consider, for instance, a general trajectory containing ℓ_1 paths of the type $-a \to 0 \to -a$ and ℓ_2 paths of the type $a \to 0 \to a$, related with the linear function $K^{(1)}$. In addition, we allow m paths of the type $-a \to a \to -a$, related with $K^{(2)}$. Then, this particular trajectory will contribute to the propagator with a term

$$K^{(\ell_1,\ell_2,m)}\left(-a, \frac{t}{2}\middle| -a, -\frac{t}{2}\right) = K^{(0)} \frac{\left(-g_0^2 t\right)^{\ell_1+\ell_2+2m}}{(\ell_1+\ell_2+2m)!} \times \Gamma^{\ell_1+\ell_2+2m}\,. \tag{5.15}$$

By carefully counting the number of different paths which contribute to each trajectory labeled by (ℓ_1, ℓ_2, m) and summing up, we finally arrive at the expression for the conditional probability,

$$P\left(-a, \frac{t}{2}\middle| -a, -\frac{t}{2}\right) = \frac{1}{2}K^{(0)}(1 + e^{-t/\tau_k}). \tag{5.16}$$

On the other hand, by using the same formalism, we easily find the expression for the conditional probability of finding the system in the state $x = a$ at time $t/2$, provided it was in

the state $x = -a$ at a previous time $-t/2$,

$$P\left(a, \frac{t}{2}\middle| -a, -\frac{t}{2}\right) = \frac{1}{2}K^{(0)}(1 - e^{-t/\tau_k}). \tag{5.17}$$

In Eqs. (5.16) and (5.17), the inverse time parameter τ_k^{-1}, which is equivalent to the Kramers escape rate, is given by $\tau_k^{-1} = r_{\text{mult}} = g_0^2\Gamma$. Using Eq. (5.13), it is explicitly written as

$$r_{\text{mult}} = g_0^2 \frac{\sqrt{U''_{\text{eq}}(a)|U''_{\text{eq}}(0)|}}{2\pi} e^{-\frac{\Delta U_{\text{eq}}}{\sigma^2}}, \tag{5.18}$$

with $\Delta U_{\text{eq}} = U_{\text{eq}}(0) - U_{\text{eq}}(a)$.

This is one of the main results of our paper. Comparing Eq. (5.18) with the classical result of Eq. (1.1), we clearly see the effect of the multiplicative noise. Notice that the role of the original potential $U(x)$ is now played by the equilibrium potential $U_{\text{eq}}(x)$ given by Eq. (2.5). This potential depends not only on the diffusion function $g(x)$ and the noise, but also on the stochastic prescription α which defines the original Langevin equation. There is also an important global scaling factor given by $g^2(0)$.

It is worth to mention that, to the best of our knowledge, there are only a few papers where analytic expressions for the escape rate in the multiplicative noise case were in fact derived. Indeed, there is not one where different stochastic prescriptions are discussed. In Refs. [28–30], particular examples combining multiplicative with additive noise were treated. There seems to be a consensus that in the exponential part of the Arrhenius form, the classical potential should be replaced by an effective potential computed from the static solution of the Fokker-Planck equation. However, the values presented for the prefactor differ from ours. In all those references, there is no indication of the discretization prescription used. This fact is quite important in multiplicative noise, since different prescriptions correspond to completely different stochastic processes. In such a situation, it is necessary to proceed with great care in order to compare analytic expressions and numerical data. In Ref. [32], a careful treatment of the first time passage was made by focusing on the Fokker-Planck equation in the Stratonovich prescription. Its result coincides with ours for $\alpha = 1/2$ in the weak noise limit.

In order to gain more insight into Eq. (5.18), let us compare the Kramers escape rate with the expression of r_{mult}, expanding Eq. (5.18) for weak noise. We obtain

$$\frac{r_{\text{mult}}}{r_{\text{add}}} = |g_0|^{2\alpha}|g_a|^{2(1-\alpha)}[1 + O(\sigma^2)]. \tag{5.19}$$

It can be noticed that the relation between both escape rates does not depend on details of $g(x)$, but on its value at each maxima of $-V(x)$, $x = \pm a$ and $x = 0$. As expected, Eq. (5.19) depends on the stochastic prescription parameter α. For instance, in the case of the Stratonovich prescription, $\alpha = 1/2$, $r_{\text{mult}}/r_{\text{add}} = g_0 g_a$. In this case, g_0 and g_a have the same weight. On the other hand, in the Itô interpretation $\alpha = 0$, $r_{\text{mult}}/r_{\text{add}} = g_a^2$ while in the thermal prescription, $\alpha = 1$, $r_{\text{mult}}/r_{\text{add}} = g_0^2$. Indeed, Eq. (5.19) is invariant under the transformation

$$\alpha \longleftrightarrow 1 - \alpha, \tag{5.20}$$

$$0 \longleftrightarrow a, \tag{5.21}$$

which is nothing but a time-reversal transformation [39]. The simplest way to understand this symmetry is by noting that the instanton solution $x_I(t)$ interpolates between the states $x = -a$ and $x = 0$. The time-reversal solution, the anti-instanton $x_A(t) = x_I(-t)$, makes the inverse trajectory, i.e., connecting $x = 0$ with $x = a$. However, if the forward time process evolves with the α prescription, the backward evolution takes place with the $1 - \alpha$ prescription. In this sense, one process is the time-reversal conjugate of the other one. For this reason, the kinetic prescription $\alpha = 1$ is also called the anti-Itô interpretation. In fact, the only time-reversal invariant prescription is the Stratonovich one, $\alpha = 1/2$. For details on the time-reversal transformation in multiplicative noise dynamics, please see Refs. [38–40].

Let us finally mention that the escape rate in the multiplicative case may be greater or lower than in the additive case, depending essentially on the values of $g(0)$ and $g(a)$. Moreover, if the diffusion function $g(x)$ locally approaches zero at either $x = a$ or $x = 0$, the escape rate goes to zero. This effect can be understood from the fact that the effective curvature of $V(x)$ approaches zero and the particle tends to remain in the well for a long time. Of course, our approximation $t \gg \tau_k$ is no longer valid in this limit.

VI. NUMERICAL SIMULATIONS

In this section, we perform numerical simulations for the stochastic process driven by the Langevin equation (2.2) with (2.3), interpreted in the *generalized Stratonovich* prescription. We use the Euler-Maruyama scheme, which is the simplest algorithm for this task. This algorithm implies an Itô discretization of the stochastic differential equation (SDE). Thus, for a Langevin equation interpreted in a given α prescription, $0 \leqslant \alpha \leqslant 1$, it must be transformed to Itô prescription by appropriately changing the drift function $f(x)$. As a consequence, we represent any α defined SDE by means of the following Itô differential equation:

$$\frac{dx}{dt} = -\frac{1}{2}g^2(x)\frac{dU(x)}{dx} + \sigma^2\alpha g(x)g'(x) + g(x)\eta(t). \tag{6.1}$$

Equation (6.1) was obtained from Eq. (2.2) by shifting $f(x) \to f(x) + \sigma^2\alpha g(x)g'(x)$ [43].

Considering the model given by Eqs. (2.6) and (2.7), we explicitly have the Itô SDE,

$$dx = \frac{x(1+\lambda x^2)}{2}[(1-x^2)(1+\lambda x^2) + 4\lambda\sigma^2\alpha]dt + (1+\lambda x^2)dW, \tag{6.2}$$

where $W(t)$ is a standard Wiener process with $\langle W(t)\rangle = 0$ and $\langle W(t)W(t')\rangle = \sigma^2\min(t, t')$. In Fig. 5, we show a typical output for a particular noise realization. Fixing the initial condition $x(0) = 1$, we clearly see the dynamics of the stochastic variable $x(t)$, fluctuating around the potential minima $x_{\text{min}} \sim \pm 1$, flipping between them at seemly irregular times.

We have computed the mean value $\langle x(t)\rangle$ over different noise realizations. In Fig. 6, we show the result of averaging over 8×10^4 configurations of the noise for different values of the stochastic prescription. We can observe that, as expected, $\langle x(t)\rangle$ tends to zero exponentially. This means that, at long times, the particle is flipping between both potential wells

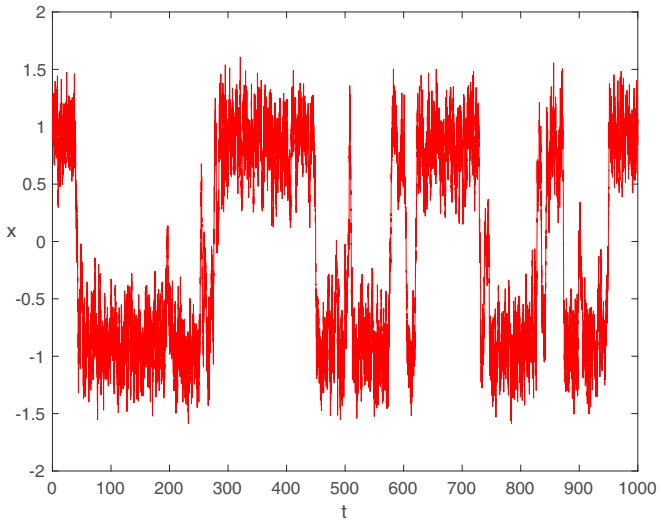

FIG. 5. $x(t)$, computed from the integration of Eq. (6.2) for a particular realization of the noise, for $\lambda = 0.5$, $\alpha = 1/2$, and $\sigma^2 = 0.095$. Time interval $0 < t < 1000$ was divided into 2×10^4 steps.

with zero mean value. We can also observe that the typical decay time is not the same for different stochastic prescriptions and, in general, $\tau_I < \tau_S < \tau_K$, where τ_I, τ_S, and τ_K are the decay times in the Itô, Stratonovich, and kinetic prescriptions. This is consistent with the fact observed in Fig. 1, where we can see that the height of the equilibrium potential barrier increases with increasing α.

By using the asymptotic conditional probability distributions, Eqs. (5.16) and (5.17), it is not difficult to show that, for $t \gg \tau_k$,

$$\langle x(t) \rangle = A\, e^{-t/\tau_k}, \tag{6.3}$$

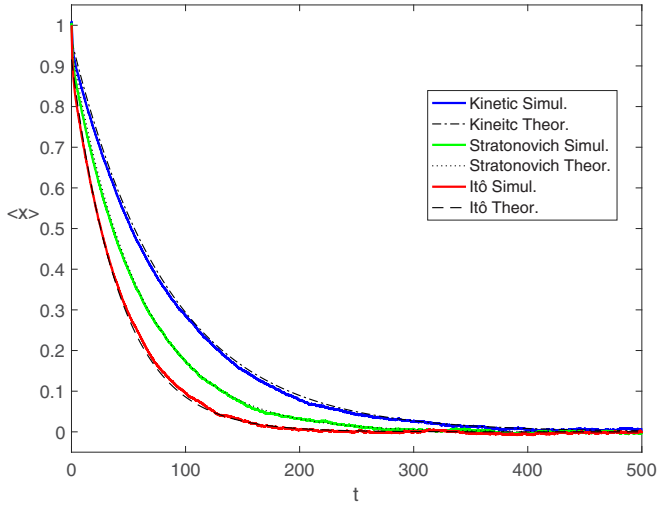

FIG. 6. $\langle x(t) \rangle$ averaged over 8×10^4 noise realizations. We fixed the initial condition $x(0) = 1$ and the parameters $\lambda = 0.5$ and $\sigma^2 = 0.085$. The three curves corresponds to three different stochastic prescriptions, $\alpha = 0, 1/2, 1$. The continuous lines are the numerical simulations while the dashed, dotted, and dash-dotted lines correspond to a theoretical fitting using Eq. (5.18), in the Itô, Stratonovich, and kinetics stochastic prescription, respectively.

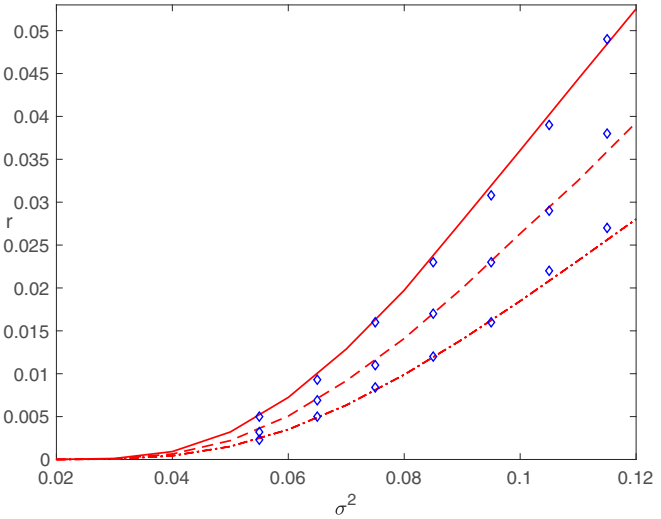

FIG. 7. Decay rate r_{mult} as a function of the noise intensity σ^2 computed using Eq. (5.18). The continuous line corresponds to the decay rate in the Itô prescription. For Stratonovich and kinetic or anti-Itô interpretations, the decay rate is depicted by the dashed and dot-dashed curves, respectively. The points (diamonds) were obtained from a linear fitting of $\ln\langle x(t) \rangle$ through numerical simulations for each case. For all the data, it was fixed $\lambda = 0.5$.

where A is some constant. We have used Eq. (6.3), with $\tau_k = r_{\text{mult}}^{-1}$ computed in Eq. (5.18), to compare the simulations and the theoretical prediction in the three cases shown in Fig. 6, obtaining excellent fittings.

In order to have more accurate results, the numerical decay rate $r = \tau_k^{-1}$ can be obtained from a linear least-square fitting of $\ln\langle x(t) \rangle$. Following this procedure, we studied a wide range of the parameter space $\{\alpha, \sigma^2\}$ and we compared the output with the analytic decay rate of Eq. (5.18). In Fig. 7, we show the decay rate r_{mult} as a function of the noise intensity σ^2 for three different values of the stochastic prescription. The continuous line represents the decay rate in the Itô prescription. The Stratonovich interpretation is depicted by the dashed line and the dot-dashed curve shows the decay rate in the kinetic or anti-Itô prescription. The diamonds are numerical results obtained by the least-square fitting of $\ln\langle x(t) \rangle$ in each case. We can observe an excellent agreement over almost all the noise range. As expected, there is a small deviation for larger values of the noise, since in these cases $\Delta U_{\text{eq}}/\sigma^2 \gtrsim 1$, and the Arrhenius form is no longer a good approximation.

In Fig. 8, we show the decay rate r_{mult} as a function of the stochastic prescription $0 \leqslant \alpha \leqslant 1$, for different values of the noise from $\sigma^2 = 0.055$ to $\sigma^2 = 0.085$. We observe an excellent agreement between the theoretical predictions and the data computed from the numerical simulation of the Langevin equation. In this figure, the continuous line was plotted fixing $\sigma^2 = 0.055$ and has a perfect match with the numerical results. We expect that lower values of the noise produce still better results. However, for these values, the time decays are huge, being on the order of $t = 1000$ for $\sigma^2 = 0.055$. So, in order to have statistics for a lower noise range, it would be necessary to simulate for much longer timescales considering a big number of noise realiza-

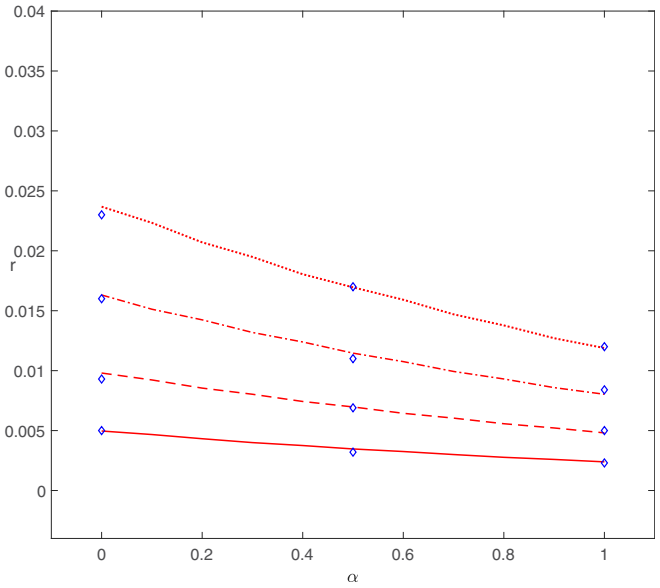

FIG. 8. Decay rate $r = \tau_k^{-1}$ as a function of the stochastic prescription α obtained from Eq. (5.18) for different values of σ^2. The continuous line is plotted for $\sigma^2 = 0.055$, dashed line corresponds to $\sigma^2 = 0.065$, while the dot-dashed and dotted lines correspond to $\sigma^2 = 0.075$ and $\sigma^2 = 0.085$, respectively. The points (diamonds) results from numerical simulation, computed by linear fittings of $\ln\langle x(t)\rangle$. Parameter $\lambda = 0.5$ was fixed for all the curves.

tions. Of course, this consumes much more computational resources.

VII. SUMMARY AND CONCLUSIONS

We have considered the problem of a particle in a symmetric double-well potential $U(x)$, with a dynamics driven by an overdamped multiplicative Langevin equation characterized by a symmetric diffusion function $g(x) = g(-x)$. The stochastic differential equation was defined in the *generalized Stratonovich* prescription, parametrized by a continuum parameter $0 \leqslant \alpha \leqslant 1$. This prescription contains the usual stochastic interpretations for particular values of the parameter α. Indeed, $\alpha = 0, 1/2, 1$ corresponds to the usual Itô, Stratonovich, and kinetic prescriptions, respectively.

We have provided a path integral technique to compute conditional probabilities in the weak noise approximation for arbitrary values of the parameter α. Interestingly, all the dependence of α is codified in the equilibrium potential $U_{\rm eq}(x)$, obtained by means of a static solution of the associated Fokker-Planck equation.

We introduced a local time reparametrization, which allows us to exactly integrate fluctuations around saddle-point solutions. Conditional probabilities were computed for long time intervals by generalizing the instanton/anti-instanton diluted gas approximation, already developed for the additive noise case [47]. From these probabilities, the escape rate was computed in the same approximation and the result was compared with the Kramers escape rate for additive noise dynamics.

The main result of the paper is given by Eq. (5.18). We found that the general structure of the escape rate keeps the Arrhenius form of the Kramers result. The main corrections are twofold. First, the equilibrium potential $U_{\rm eq}(x)$ of Eq. (2.5) plays the role of the bare potential $U(x)$. The potential $U_{\rm eq}(x)$ is generally different from $U(x)$ in the multiplicative noise case, depending on the diffusion function and the stochastic prescription α. Indeed, the only stochastic prescription in which $U_{\rm eq}(x) = U(x)$ is the anti-Itô prescription $\alpha = 1$. Moreover, there is a global scale factor $g^2(0)$ that has its origin in the time reparametrization necessary to correctly compute fluctuations.

In the weak noise limit, we found a simple relation between the Kramers escape rates computed with additive and multiplicative noise, given by Eq. (5.19). The obvious consistency check is that $r_{\rm mult}/r_{\rm add} = 1$ in the limit $g(x) \to 1$ (or $\lambda \to 0$ in the particular example). In addition, we observe that $g(0)$ and $g(a)$ enter with different weights depending on the prescription parameter α. These weights are consistent with a time-reversal transformation, which relates a stochastic process in the α prescription with its time reversal conjugate $1 - \alpha$. Indeed, the Stratonovich convention $\alpha = 1/2$ is the only one with time-reversal invariance and, in this case, both maxima enter with the same weight.

Finally, we have made extensive Langevin simulations to test the accuracy of our expressions. We have explored a huge region of the parameter space $\{\sigma, \alpha\}$, in which the high barrier approximation, $\Delta U_{\rm eq}/\sigma^2 \gg 1$, is well defined. We have found a very good agreement for all values of the stochastic prescription.

Although we have presented results for a system with full reflection symmetry $x \to -x$, the methods developed in this paper are completely general. We hope to communicate results for a more general nonsymmetric case in the near future. Moreover, by having analytic expressions for the conditional probability we can face the problem of stochastic resonance in multiplicative noise processes in a more solid basis.

ACKNOWLEDGMENTS

The Brazilian agencies, Fundação de Amparo à Pesquisa do Rio de Janeiro (FAPERJ), Conselho Nacional de Desenvolvimento Científico e Tecnológico (CNPq), and Coordenação de Aperfeiçoamento de Pessoal de Nível Superior (CAPES), Finance Code No. 001, are acknowledged for partial financial support. M.V.M. is partially supported by CNPq through a postdoctoral fellowship.

APPENDIX: ZERO MODES IN THE MULTIPLICATIVE CASE

The relation of zero modes of the fluctuation operator and translation invariance is very well known in quantum mechanics [45], as well as in additive noise stochastic dynamics [47]. In this Appendix, we focus on the effect produced by the diffusion function $g(x)$ in a multiplicative noise stochastic system.

Let us consider the instanton function $x_I(t)$ as a solution of the equation of motion, Eq. (4.1), with boundary conditions $\lim_{t\to-\infty} x_I(t) = -a$ and $\lim_{t\to\infty} x_I(t) = 0$, where $-a$ and 0 are the positions of a minimum and the local maximun of

$U_{\rm eq}(x)$, respectively. In the weak noise approximation, these values coincide with two local maxima of $-V(x)$ as shown in Fig. 2. It is not difficult to show that dx_I/dt is a zero mode of the fluctuation operator Eq. (4.8). To see this, we consider

$$\begin{aligned}\int dt' O(t,t')\frac{dx_I(t')}{dt'} &= -\frac{d}{dt}\left(\frac{1}{g^2}\frac{d^2x_I}{dt^2}\right)+\left(\frac{1}{g^2}V'_{\rm eff}\right)'\frac{dx_I}{dt}\\ &= -\frac{d}{dt}\left(\frac{1}{g^2}V'_{\rm eff}\right)+\left(\frac{1}{g^2}V'_{\rm eff}\right)'\frac{dx_I}{dt}=0, \end{aligned} \tag{A1}$$

where in the first term of the last line we have used $d^2x_I/dt^2 = V_{\rm eff}$ and in the second term we used the chain rule.

Thus, the fluctuation operator has a normalized zero mode of the form

$$\eta_0(t) = A\frac{dx_I(t)}{dt}\,, \tag{A2}$$

where A is a normalization constant. To determine it, we impose

$$\int dt\ \eta_0^2(t) = A^2\int dt\left(\frac{dx_I}{dt}\right)^2 = 1 \tag{A3}$$

and, thus, the normalization constant reads

$$A^{-2} = \int dt\left(\frac{dx_I}{dt}\right)^2. \tag{A4}$$

The action computed at the instanton solution is

$$S_I = \int dt\left\{\frac{1}{2g^2(x_I)}\left(\frac{dx_I}{dt}\right)^2 + V(x_I)\right\}. \tag{A5}$$

Using the equations of motion, it can be written as

$$S_I = \int dt\ \frac{1}{g^2(x_I)}\left(\frac{dx_I}{dt}\right)^2. \tag{A6}$$

Since the zero mode has a small support around t_0, in the thin-wall approximation we can write with good accuracy

$$S_I \sim \frac{1}{g_a^2}\int dt\left(\frac{dx_I}{dt}\right)^2, \tag{A7}$$

where $g_a = g(a)$. Replacing this result in Eq. (A4) we finally find the normalized zero mode

$$\eta_0(t) = \frac{1}{g_a\sqrt{S_I}}\frac{dx_I(t)}{dt}. \tag{A8}$$

In order to compute fluctuations, we perform a local time reparametrization given by Eq. (4.10). We are led to the computation of the integral

$$I_F = \int [\mathcal{D}\delta x]\ e^{-\frac{1}{2}\int d\tau\delta x(\tau)\left(-\frac{d^2}{d\tau^2}+W[x_{cl}]\right)\delta x(\tau)}\,, \tag{A9}$$

where W is given by Eq. (4.12). To compute it, we expand fluctuations in eigenfunctions of the fluctuation operator, taking special care with the translational modes that are responsible for the zero mode. We write the fluctuation field in the following form:

$$\delta x(\tau) = c_0\psi_0(\tau-\tau_0) + \sum_{k=1}^{\infty} c_k\psi_k(\tau-\tau_0), \tag{A10}$$

where ψ_k are eigenvectors

$$\left(-\frac{d^2}{d\tau^2}+W[x_{cl}]\right)\psi_n(\tau) = \lambda_n\psi_n(\tau) \tag{A11}$$

with eigenvalues $\lambda_k \neq 0$ and the zero mode in the reparametrized variable reads

$$\psi_0(\tau) = \frac{1}{g_a\sqrt{S_I}}\ g^2(x_I(\tau))\frac{dx_I(\tau)}{d\tau}\,. \tag{A12}$$

The functional measure can be written in terms of the coefficients c_k as

$$\mathcal{D}\delta x = dc_0\prod_{k\neq 0} dc_k\,. \tag{A13}$$

Computing the variation of fluctuations under time translation, we have that

$$d\delta x(\tau) = \frac{dx_I}{d\tau}d\tau_0\,. \tag{A14}$$

On the other hand, a variation in the zero mode reads

$$d\delta x(\tau) = \frac{1}{g_a\sqrt{S_I}}\ g^2(x_I(\tau))\frac{dx_I}{d\tau}dc_0\,. \tag{A15}$$

Now, comparing Eqs. (A14) and (A15) and using the reparametrization identity $d\tau/dt = g^2(x_I)$, we immediately find

$$dc_0 = g_a\sqrt{S_I}dt_0\,. \tag{A16}$$

In this way,

$$\begin{aligned} I_F &= \int g_a\sqrt{S_I}dt_0\int\left(\prod_{k\neq 0}dc_k\right)\exp\left[-\frac{1}{2}\sum_n\lambda_n(\tau_0)c_n^2\right]\\ &= \int g_a\sqrt{S_I}dt_0\left[\prod_{k\neq 0}\lambda_k^{-1/2}(\tau_0)\right]\\ &= \int dt_0\ g_a\sqrt{S_I}\left[\det{}'\left(-\frac{d^2}{d\tau^2}+W[x_{cl}]\right)\right]^{-1/2}, \end{aligned} \tag{A17}$$

where the prime means that the determinant should be computed without the zero mode.

Thus, the usual interpretation of the zero mode as an integration in the collective variable dt_0 is still valid in the multiplicative case. However, the constant of proportionality is renormalized by the diffusion function g_a, computed at the minimum of the potential.

The same reasoning applies to the anti-instanton solutions. However, in this case, the variation is proportional to $g_0\sqrt{S_A}dt_1$, where g_0 is evaluated at the maximum of the potential and S_A is the classical action evaluated at the anti-instanton solution. This analysis leads to Eq. (5.11) for $K^{(1)}$.

[1] G. R. Fleming and P. Hänggi, *Activated Barrier Crossing: Applications In Physics, Chemistry And Biology*, Advanced Database Research and Development Series (World Scientific, Singapore, 1993).

[2] H. Kramers, Phys. (Amsterdam, Neth.) **7**, 284 (1940).

[3] P. Hänggi, P. Talkner, and M. Borkovec, Rev. Mod. Phys. **62**, 251 (1990).

[4] A. J. Bray and A. J. McKane, Phys. Rev. Lett. **62**, 493 (1989).

[5] A. J. McKane, H. C. Luckock, and A. J. Bray, Phys. Rev. A **41**, 644 (1990).

[6] A. J. Bray, A. J. McKane, and T. J. Newman, Phys. Rev. A **41**, 657 (1990).

[7] H. C. Luckock and A. J. McKane, Phys. Rev. A **42**, 1982 (1990).

[8] P. Jung, A. Neiman, M. K. N. Afghan, S. Nadkarni, and G. Ullah, New J. Phys. **7**, 17 (2005).

[9] D. Goulding, S. Melnik, D. Curtin, T. Piwonski, J. Houlihan, J. P. Gleeson, and G. Huyet, Phys. Rev. E **76**, 031128 (2007).

[10] P. Lançon, G. Batrouni, L. Lobry, and N. Ostrowsky, Europhys. Lett. **54**, 28 (2001).

[11] P. Lançon, G. Batrouni, L. Lobry, and N. Ostrowsky, Phys. A (Amsterdam, Neth.) **304**, 65 (2002).

[12] A. W. C. Lau and T. C. Lubensky, Phys. Rev. E **76**, 011123 (2007).

[13] G. Volpe, L. Helden, T. Brettschneider, J. Wehr, and C. Bechinger, Phys. Rev. Lett. **104**, 170602 (2010).

[14] T. Brettschneider, G. Volpe, L. Helden, J. Wehr, and C. Bechinger, Phys. Rev. E **83**, 041113 (2011).

[15] J. L. García-Palacios and F. J. Lázaro, Phys. Rev. B **58**, 14937 (1998).

[16] C. Aron, D. G. Barci, L. F. Cugliandolo, Z. G. Arenas, and G. S. Lozano, J. Stat. Mech.: Theory Exp. (2014) P09008.

[17] G. Arenas, D. G. Barci, and M. V. Moreno, Phys. A (Amsterdam, Neth.) **510**, 98 (2018).

[18] H. Hinrichsen, Adv. Phys. **49**, 815 (2000).

[19] C. Van den Broeck, J. M. R. Parrondo, and R. Toral, Phys. Rev. Lett. **73**, 3395 (1994).

[20] F. Castro, A. D. Sánchez, and H. S. Wio, Phys. Rev. Lett. **75**, 1691 (1995).

[21] O. Carrillo, M. Ibañes, J. García-Ojalvo, J. Casademunt, and J. M. Sancho, Phys. Rev. E **67**, 046110 (2003).

[22] F. Jafarpour, T. Biancalani, and N. Goldenfeld, Phys. Rev. Lett. **115**, 158101 (2015).

[23] D. G. Barci, Z. G. Arenas, and M. V. Moreno, Europhys. Lett. **113**, 10009 (2016).

[24] R. Benzi, A. Sutera, and A. Vulpiani, J. Phys. A: Math. Gen. **14**, L453 (1981).

[25] R. Benzi, G. Parisi, A. Sutera, and A. Vulpiani, SIAM J. Appl. Math. **43**, 565 (1983).

[26] H. S. Wio and R. R. Deza, Eur. Phys. J.: Spec. Top. **146**, 111 (2007).

[27] H. Wio, S. Bouzat, and B. von Haeften, Phys. A (Amsterdam, Neth.) **306**, 140 (2002).

[28] Y. Jin, W. Xu, and M. Xu, Chaos Solitons Fractals **26**, 1183 (2005).

[29] F. Guo and X.-F. Cheng, J. Korean Phys. Soc. **58**, 1567 (2011).

[30] N. Li-Juan and X. Wei, Chin. Phys. Lett. **23**, 3180 (2006).

[31] X.-D. Zheng, X.-Q. Yang, and Y. Tao, PLoS One **6**, e17104 (2011).

[32] A. Rosas, I. L. D. Pinto, and K. Lindenberg, Phys. Rev. E **94**, 012101 (2016).

[33] D. A. Sivak, J. D. Chodera, and G. E. Crooks, Phys. Rev. X **3**, 011007 (2013).

[34] N. Goldenfeld, *Lectures on Phase Transitions and the Renormalization Group,* Frontiers in Physics Vol. 85 (Perseus, New York, 1992).

[35] H. Wio, *Path Integrals for Stochastic Processes: An Introduction* (World Scientific, Singapore, 2013).

[36] C. Aron, G. Biroli, and L. F. Cugliandolo, J. Stat. Mech.: Theory Exp. (2010) P11018.

[37] Z. G. Arenas and D. G. Barci, Phys. Rev. E **81**, 051113 (2010).

[38] Z. G. Arenas and D. G. Barci, Phys. Rev. E **85**, 041122 (2012).

[39] Z. G. Arenas and D. G. Barci, J. Stat. Mech.: Theory Exp. (2012) P12005.

[40] M. V. Moreno, Z. G. Arenas, and D. G. Barci, Phys. Rev. E **91**, 042103 (2015).

[41] C. Aron, D. G. Barci, L. F. Cugliandolo, Z. G. Arenas, and G. S. Lozano, J. Stat. Mech.: Theory Exp. (2016) 053207.

[42] H. K. Janssen, *From Phase Transitions to Chaos: Topics in Modern Statistical Physics* (World Scientific, Singapore, 1992).

[43] M. V. Moreno, D. G. Barci, and Z. G. Arenas, Phys. Rev. E **99**, 032125 (2019).

[44] J. Zinn-Justin, *Quantum Field Theory and Critical Phenomena* (Oxford University Press, New York, 2002).

[45] S. Coleman, "The uses of instantons", in *The Whys of Subnuclear Physics*, edited by A. Zichichi (Springer, Boston, 1979), pp. 805–941.

[46] B. Caroli, C. Caroli, and B. Roulet, J. Stat. Phys. **21**, 415 (1979).

[47] B. Caroli, C. Caroli, and B. Roulet, J. Stat. Phys. **26**, 83 (1981).

[48] P. Hänggi, Helv. Phys. Acta **51**, 183 (1978).

[49] P. Hänggi and H. Thomas, Phys. Rep. **88**, 207 (1982).

[50] Y. L. Klimontovich, Phys. Usp. **37**, 737 (1994).

[51] E. Brézin, G. Parisi, and J. Zinn-Justin, Phys. Rev. D **16**, 408 (1977).

[52] E. Bogomolny, Phys. Lett. B **91**, 431 (1980).

[53] G. V. Dunne, J. Phys. A: Math. Theor. **41**, 304006 (2008).